

Electronic Supporting Information

Hydrogen Peroxide as a Hydride Donor and Reductant under Biologically Relevant Conditions

Yamin Htet,^{ab} Zhuomin Lu,^d Sunia A. Trauger,^c and Andrew G. Tennyson^{*def}

^a Wyss Institute for Biologically Inspired Engineering, ^b John A. Paulson School of Engineering and Applied Sciences, ^c Harvard FAS Small Molecule Mass Spectrometry Facility, Harvard University, Cambridge, MA 02138, USA

^d Departments of Chemistry and ^e Materials Science and Engineering, Clemson University, Clemson, SC 29634, USA

^f Center for Optical Materials Science and Engineering Technologies, Anderson, SC 29625, USA

E-mail: atennys@clemson.edu

Table of Contents

Synthetic Procedures	S2
Spectroscopic and Kinetic Analysis Procedures	S2
Derivation of General Rate Law for Proposed Mechanism	S4
Figure S1. UV/vis of ABTS ²⁻ formed from reduction of ABTS ⁻	S8
Figure S2. Digital images from volumetric O ₂ gas evolution experiments	S9
Figure S3. UV/vis of aliquots from volumetric O ₂ gas evolution experiments	S11
Figure S4. Direct-inject ESI-MS of Ru1 -catalyzed ABTS ⁻ reduction	S12
References	S13

Synthetic Procedures

General synthetic considerations. The compounds **Ru1** and ABTS^{•-} were prepared and measured as previously described.¹⁻³ All other materials were of reagent quality and used as received. All solvents used were HPLC grade. ¹H and ¹³C{¹H} NMR spectra were recorded using a Bruker 500 MHz spectrometer. Chemical shifts δ (in ppm) for ¹H and ¹³C NMR are referenced to SiMe₄ using the residual protio-solvent as an internal standard. For ¹H NMR: CDCl₃, 7.26 ppm; DMSO-*d*₆, 2.50 ppm. For ¹³C NMR: CDCl₃, 77.16 ppm; DMSO-*d*₆, 39.52 ppm. Coupling constants (*J*) are expressed in hertz (Hz). Fourier transform high-resolution mass spectrometry with electrospray ionization (ESI-MS) were acquired on a Thermo q-Exactive Plus instrument via direct injection (100% CH₃CN) using a Thermo Ultimate 3000 HPLC at a flow rate of 0.2L/min. A resolving power of 140,000 was used for the data acquisition, and the instrument was calibrated immediately prior to use yielding better than 5 ppm mass accuracy. All reactions were performed under an inert atmosphere under an N₂ atmosphere using standard Schlenk or glovebox techniques with the exclusion of light. All subsequent manipulations were performed under ambient conditions using standard benchtop techniques without the exclusion of light. When required, solvents were dried and deoxygenated using an Innovative Technologies solvent purification system, and then stored over molecular sieves (3 Å) in a drybox.

Spectroscopic and Kinetic Analysis Procedures

General spectroscopic considerations. UV-visible absorption spectra were acquired on a Varian Cary 50 Bio spectrometer equipped with a water-cooled Quantum Northwest TC-125 peltier temperature controller. All solution measurements were performed at 25.0 ± 0.1 °C in matched gas-tight quartz cuvettes (Precision Scientific) with 1 cm path lengths and 3.0 mL analyte solution volumes. Absorption spectra were acquired from 950 to 200 nm with a scanning speed of 300 nm min⁻¹ and a resolution of 0.5 nm. Each kinetic analysis experiment (5 second intervals) was performed in quadruplicate on four different days. Stock solutions were prepared fresh daily and filtered (0.2 μm PTFE) immediately prior to use.

General kinetic procedure for analysis of ABTS^{•-} degradation by Ru1 in PBS. This procedure was used to generate the data for Figure 1. An aliquot of ABTS²⁻ (30 μL from stock solution in H₂O) and an aliquot of ABTS^{•-} (35 μL from stock solution in H₂O) were added to PBS (pH 7.4) and this working solution was allowed to equilibrate at 25 °C for 10 min. The absorbance spectrum of this working solution was acquired to confirm ABTS^{•-} concentration and the single wavelength kinetics program was initiated. After 20 s, the cuvette was removed from the spectrometer without stopping the kinetics program, an aliquot of **Ru1** (30 μL from stock solution in CH₃CN) was added, the cuvette was covered and mixed via repeated inversion for 3 s, placed back in the spectrometer, and the kinetics program was allowed to continue. After 5 min, an aliquot of 100 μM H₂O₂, *t*-Bu₂O₂, or *t*-BuOOH (30 μL from stock solution in H₂O) was added, the cuvette was covered and mixed via repeated inversion for 3 s, placed back in the spectrometer, and the kinetics program was allowed to continue. After the kinetics program had completed, the absorbance spectrum was acquired to confirm the formation of ABTS²⁻ from the peak at 340 nm. **Standard Conditions** (unless specified otherwise): 100 μM ABTS²⁻, 50 μM ABTS^{•-}, 5 μM **Ru1**, 100 μM H₂O₂, *t*-Bu₂O₂, or *t*-BuOOH, PBS (pH 7.4), 25 °C; [ABTS^{•-}] determined from the absorbance at 734 nm, [ABTS²⁻] determined from the absorbance at 340 nm. **Notes:** (i) A 100 μM aliquot of ABTS²⁻ is added at the beginning of each experiment to ensure initial ABTS²⁻/**Ru1** ratios are consistent across different experimental conditions. (ii) ABTS^{•-} reduction is incomplete after 30 min under these conditions due to the large (i.e., >20:1) ABTS²⁻/**Ru1** ratios and the fact that ABTS²⁻ inhibits **Ru1**-catalyzed ABTS^{•-} reduction.²

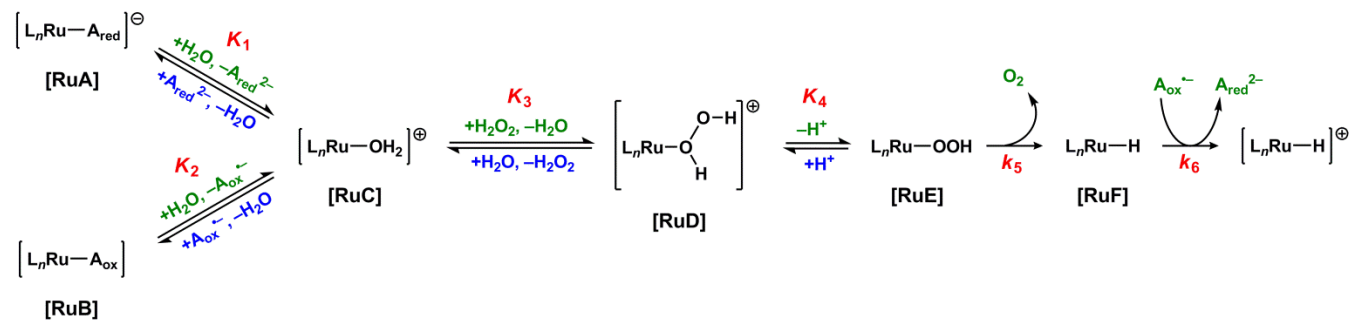
Quantitative ABTS^{•-} reduction to ABTS²⁻ experiments. This procedure was used to generate the data for Figure S1. The concentrations of ABTS^{•-}, **Ru1**, and H₂O₂ employed in these experiments were obtained by using the general kinetic procedure and standard conditions, holding aliquot volumes constant but varying stock solution concentrations. A 100 μM aliquot of ABTS²⁻ was not added at the beginning of this experiment because the combined absorbance of this initial aliquot and the ABTS²⁻ formed during the reaction would saturate the detector and prevent quantification of [ABTS²⁻]. Note: ABTS^{•-} reduction is complete after 30 min at 25 °C without an initial 100 μM aliquot of ABTS²⁻ due to smaller ABTS²⁻/**Ru1** ratios.

Volumetric quantification of O₂ gas evolution. This procedure was used to generate data for Figure S3. The concentrations of ABTS^{•-}, **Ru1**, and H₂O₂ employed in these experiments were obtained by using the general kinetic procedure and standard conditions, holding stock solution concentrations constant and varying aliquot volumes to achieve a final volume of 3.00 L. A 100 μM aliquot of ABTS²⁻ was not added at the beginning of this experiment because the combined absorbance of this initial aliquot and the ABTS²⁻ formed during the reaction would saturate the detector and prevent quantification of [ABTS²⁻]. Note: ABTS^{•-} reduction is incomplete after 30 min at 19 °C without an initial 100 μM aliquot of ABTS²⁻ due to the lower temperature (i.e., 19 °C temperature in the flask in the hood vs. 25 °C in the Peltier-controlled cuvette holder).

Rate law experiments. This procedure was used to generate the data for Figure 4. The concentrations of ABTS²⁻, ABTS^{•-}, **Ru1**, and H₂O₂ employed in these experiments were obtained by using the general kinetic procedure and standard conditions, holding aliquot volumes constant but varying stock solution concentrations. The H⁺ concentrations were obtained using PBS adjusted to different pH values before the addition of any aliquots. The temperatures were obtained by allowing the working solution to equilibrate at different temperatures before the addition of **Ru1**. Note: A 100 μM aliquot of ABTS²⁻ is added at the beginning of each experiment to ensure initial ABTS²⁻/**Ru1** ratios are consistent across different experimental conditions.²

Kinetic isotope effect experiments. The general kinetic procedure and standard conditions were employed as described for the rate law experiments, with minor modifications. Kinetic isotope effect experiments were performed in either protio PBS (pH 7.4) or deuterio PBS (pD 7.4). Stock solutions of H₂O₂ and D₂O₂ (5.0 M) were prepared in H₂O and D₂O, respectively.

Derivation of General Rate Law for Proposed Mechanism



Proposed mechanism. Adapted from Scheme 2 in the manuscript. The intermediates $[L_nRu-A_{red}]^{1-}$, $[L_nRu-A_{ox}]$, $[L_nRu-OH_2]^{1+}$, $[L_nRu-(H_2O_2)]^{1+}$, $[L_nRu-OOH]$ and $[L_nRu-H]$ have been abbreviated in the following equations as [RuA], [RuB], [RuC], [RuD], [RuE], and [RuF], respectively, for clarity.

(Equation S1) Based on previous mechanistic studies, it is known that the underlying reaction is the oxidation of $[L_nRu-H]$ by ABTS^{•-}:

$$\text{rate} = -\frac{d[A_{ox}]}{dt} = k_6[A_{ox}][RuF]$$

(Equation S2) The sum of the concentrations of the Ru-containing species leading up to the rate-determining step is equal to the total concentration of **Ru1** added at the beginning of the experiment:

$$[Ru1]_0 = [RuA] + [RuB] + [RuC] + [RuD] + [RuE] + [RuF]$$

(Equation S3) Assuming that steps 1-4 achieve equilibrium rapidly (with respect to turnover):

$$K_1 = \frac{[RuC][A_{red}]}{[RuA]} \quad K_2 = \frac{[RuC][A_{ox}]}{[RuB]}$$

$$K_3 = \frac{[RuD]}{[RuC][H_2O_2]} \quad K_4 = \frac{[RuE][H^+]}{[RuD]}$$

(Equation S4) Assuming the system achieves steady-state rapidly (with respect to turnover):

$$\frac{d[RuF]}{dt} = k_5[RuE] - k_6[A_{ox}][RuF]$$

$$[RuE] = \frac{k_6[A_{ox}]}{k_5} [RuF]$$

(Equation S5) Solving Equation S2 for **[RuF]** using the relationships established in Equations S3 and S4:

$$[\mathbf{Ru1}]_0 = \left(\frac{[\mathbf{A}_{red}]}{K_1} + \frac{[\mathbf{A}_{ox}]}{K_2} \right) [\mathbf{RuC}] + [\mathbf{RuD}] + [\mathbf{RuE}] + [\mathbf{RuF}]$$

$$[\mathbf{Ru1}]_0 = \left(\frac{[\mathbf{A}_{red}]}{K_1 K_3 [\text{H}_2\text{O}_2]} + \frac{[\mathbf{A}_{ox}]}{K_2 K_3 [\text{H}_2\text{O}_2]} + \frac{1}{K_3 [\text{H}_2\text{O}_2]} + 1 \right) [\mathbf{RuD}] + [\mathbf{RuE}] + [\mathbf{RuF}]$$

$$[\mathbf{Ru1}]_0 = \left(\frac{[\mathbf{A}_{red}][\text{H}^+]}{K_1 K_3 K_4 [\text{H}_2\text{O}_2]} + \frac{[\mathbf{A}_{ox}][\text{H}^+]}{K_2 K_3 K_4 [\text{H}_2\text{O}_2]} + \frac{[\text{H}^+]}{K_3 K_4 [\text{H}_2\text{O}_2]} + \frac{[\text{H}^+]}{K_4} + 1 \right) [\mathbf{RuE}] + [\mathbf{RuF}]$$

$$[\mathbf{Ru1}]_0 = \left(\frac{k_6 [\text{H}^+] [\mathbf{A}_{red}] [\mathbf{A}_{ox}]}{k_5 K_1 K_3 K_4 [\text{H}_2\text{O}_2]} + \frac{k_6 [\text{H}^+] [\mathbf{A}_{ox}]^2}{k_5 K_2 K_3 K_4 [\text{H}_2\text{O}_2]} + \frac{k_6 [\text{H}^+] [\mathbf{A}_{ox}]}{k_5 K_3 K_4 [\text{H}_2\text{O}_2]} + \frac{k_6 [\text{H}^+] [\mathbf{A}_{ox}]}{k_5 K_4} + \frac{k_6 [\mathbf{A}_{ox}]}{k_5} + 1 \right) [\mathbf{RuF}]$$

$$[\mathbf{Ru1}]_0 = \left(\frac{k_6 K_2 [\text{H}^+] [\mathbf{A}_{red}] [\mathbf{A}_{ox}] + k_6 K_1 [\text{H}^+] [\mathbf{A}_{ox}]^2 + k_6 K_1 K_2 [\text{H}^+] [\mathbf{A}_{ox}] + k_6 K_1 K_2 K_3 [\text{H}_2\text{O}_2] [\text{H}^+] [\mathbf{A}_{ox}] + k_6 K_1 K_2 K_3 K_4 [\text{H}_2\text{O}_2] [\mathbf{A}_{ox}] + k_5 K_1 K_2 K_3 K_4 [\text{H}_2\text{O}_2]}{k_5 K_1 K_2 K_3 K_4 [\text{H}_2\text{O}_2]} \right) [\mathbf{RuF}]$$

$$[\mathbf{RuF}] = \left(\frac{k_5 K_1 K_2 K_3 K_4 [\text{H}_2\text{O}_2]}{k_6 K_2 [\text{H}^+] [\mathbf{A}_{red}] [\mathbf{A}_{ox}] + k_6 K_1 [\text{H}^+] [\mathbf{A}_{ox}]^2 + k_6 K_1 K_2 [\text{H}^+] [\mathbf{A}_{ox}] + k_6 K_1 K_2 K_3 [\text{H}_2\text{O}_2] [\text{H}^+] [\mathbf{A}_{ox}] + k_6 K_1 K_2 K_3 K_4 [\text{H}_2\text{O}_2] [\mathbf{A}_{ox}] + k_5 K_1 K_2 K_3 K_4 [\text{H}_2\text{O}_2]} \right) [\mathbf{Ru1}]_0$$

(Equation S6) Plugging the result from Equation S5 into Equation S1 gives the general rate law for the proposed mechanism:

$$\text{rate} = -\frac{d[\mathbf{A}_{\text{ox}}]}{dt} = k_6[\mathbf{A}_{\text{ox}}][\mathbf{RuF}]$$

$$= k_6[\mathbf{A}_{\text{ox}}] \left\{ \left(\frac{k_5 K_1 K_2 K_3 K_4 [\text{H}_2\text{O}_2]}{k_6 K_2 [\text{H}^+][\mathbf{A}_{\text{red}}][\mathbf{A}_{\text{ox}}] + k_6 K_1 [\text{H}^+][\mathbf{A}_{\text{ox}}]^2 + k_6 K_1 K_2 [\text{H}^+][\mathbf{A}_{\text{ox}}] + k_6 K_1 K_2 K_3 [\text{H}_2\text{O}_2][\text{H}^+][\mathbf{A}_{\text{ox}}] + k_6 K_1 K_2 K_3 K_4 [\text{H}_2\text{O}_2][\mathbf{A}_{\text{ox}}] + k_5 K_1 K_2 K_3 K_4 [\text{H}_2\text{O}_2]} \right) [\mathbf{Ru1}]_0 \right\}$$

$$= \frac{k_5 k_6 K_1 K_2 K_3 K_4 [\text{H}_2\text{O}_2][\mathbf{A}_{\text{ox}}][\mathbf{Ru1}]_0}{k_6 K_2 [\text{H}^+][\mathbf{A}_{\text{red}}][\mathbf{A}_{\text{ox}}] + k_6 K_1 [\text{H}^+][\mathbf{A}_{\text{ox}}]^2 + k_6 K_1 K_2 [\text{H}^+][\mathbf{A}_{\text{ox}}] + k_6 K_1 K_2 K_3 [\text{H}_2\text{O}_2][\text{H}^+][\mathbf{A}_{\text{ox}}] + k_6 K_1 K_2 K_3 K_4 [\text{H}_2\text{O}_2][\mathbf{A}_{\text{ox}}] + k_5 K_1 K_2 K_3 K_4 [\text{H}_2\text{O}_2]}$$

(Equation S7) At very short reaction times, the concentration of species will be very close to their initial concentrations (e.g., $[\mathbf{A}_{\text{ox}}] \approx [\mathbf{A}_{\text{ox}}]_0$), therefore the initial rate (v_0) can be expressed with the following equation:

$$v_0 = \frac{k_5 k_6 K_1 K_2 K_3 K_4 [\text{H}_2\text{O}_2]_0 [\mathbf{A}_{\text{ox}}]_0 [\mathbf{Ru1}]_0}{k_6 K_2 [\text{H}^+]_0 [\mathbf{A}_{\text{red}}]_0 [\mathbf{A}_{\text{ox}}]_0 + k_6 [\mathbf{A}_{\text{ox}}]_0^2 + k_6 K_1 K_2 [\text{H}^+]_0 [\mathbf{A}_{\text{ox}}]_0 + k_6 K_1 K_2 K_3 [\text{H}_2\text{O}_2]_0 [\text{H}^+]_0 [\mathbf{A}_{\text{ox}}]_0 + k_6 K_1 K_2 K_3 K_4 [\text{H}_2\text{O}_2]_0 [\mathbf{A}_{\text{ox}}]_0 + k_5 K_1 K_2 K_3 K_4 [\text{H}_2\text{O}_2]_0}$$

(Equation S8) The equation in (7) can be expressed in terms of the different variables $[\mathbf{A}_{\text{ox}}]_0$, $[\mathbf{A}_{\text{red}}]_0$, $[\text{H}^+]_0$, $[\text{H}_2\text{O}_2]_0$, and $[\mathbf{Ru1}]_0$ to simplify graphical analysis and data fitting:

(a) If $[\mathbf{A}_{\text{ox}}]_0$ is varied and the other variables are held constant, a plot of v_0 vs. $[\mathbf{A}_{\text{ox}}]_0$ should fit the following equation:

$$v_0 = \frac{(k_5 k_6 K_1 K_2 K_3 K_4 [\text{H}_2\text{O}_2]_0 [\mathbf{Ru1}]_0) \cdot [\mathbf{A}_{\text{ox}}]_0}{(k_6) \cdot [\mathbf{A}_{\text{ox}}]_0^2 + (k_6 K_2 [\text{H}^+]_0 [\mathbf{A}_{\text{red}}]_0 + k_6 K_1 K_2 [\text{H}^+]_0 + k_6 K_1 K_2 K_3 [\text{H}_2\text{O}_2]_0 [\text{H}^+]_0 + k_6 K_1 K_2 K_3 K_4 [\text{H}_2\text{O}_2]_0) \cdot [\mathbf{A}_{\text{ox}}]_0 + k_5 K_1 K_2 K_3 K_4 [\text{H}_2\text{O}_2]_0}$$

$$v_0 = \frac{C_1 \cdot [\mathbf{A}_{\text{ox}}]_0}{C_2 \cdot [\mathbf{A}_{\text{ox}}]_0^2 + C_3 \cdot [\mathbf{A}_{\text{ox}}]_0 + C_4}$$

(b) If $[\mathbf{A}_{\text{red}}]_0$ is varied and the other variables are held constant, a plot of v_0 vs. $[\mathbf{A}_{\text{red}}]_0$ should fit the following equation:

$$v_0 = \frac{(k_5 k_6 K_1 K_2 K_3 K_4 [\text{H}_2\text{O}_2]_0 [\mathbf{Ru1}]_0 [\mathbf{A}_{\text{ox}}]_0)}{(k_6 K_2 [\text{H}^+]_0 [\mathbf{A}_{\text{ox}}]_0) \cdot [\mathbf{A}_{\text{red}}]_0 + (k_6 [\mathbf{A}_{\text{ox}}]_0^2 + k_6 K_1 K_2 [\text{H}^+]_0 [\mathbf{A}_{\text{ox}}]_0 + k_6 K_1 K_2 K_3 [\text{H}_2\text{O}_2]_0 [\text{H}^+]_0 [\mathbf{A}_{\text{ox}}]_0 + k_6 K_1 K_2 K_3 K_4 [\text{H}_2\text{O}_2]_0 [\mathbf{A}_{\text{ox}}]_0 + k_5 K_1 K_2 K_3 K_4 [\text{H}_2\text{O}_2]_0)}$$

$$v_0 = \frac{C_5}{C_6 \cdot [\mathbf{A}_{\text{red}}]_0 + C_7}$$

(c) If $[\text{H}^+]_0$ is varied and the other variables are held constant, a plot of v_0 vs. $[\text{H}^+]_0$ should fit the following equation:

$$v_0 = \frac{(k_5 k_6 K_1 K_2 K_3 K_4 [\text{H}_2\text{O}_2]_0 [\mathbf{A}_{\text{ox}}]_0 [\mathbf{Ru1}]_0)}{(k_6 K_2 [\mathbf{A}_{\text{red}}]_0 [\mathbf{A}_{\text{ox}}]_0 + k_6 K_1 K_2 [\mathbf{A}_{\text{ox}}]_0 + k_6 K_1 K_2 K_3 [\text{H}_2\text{O}_2]_0 [\mathbf{A}_{\text{ox}}]_0) \cdot [\text{H}^+]_0 + (k_6 [\mathbf{A}_{\text{ox}}]_0^2 + k_6 K_1 K_2 K_3 K_4 [\text{H}_2\text{O}_2]_0 [\mathbf{A}_{\text{ox}}]_0 + k_5 K_1 K_2 K_3 K_4 [\text{H}_2\text{O}_2]_0)}$$

$$v_0 = \frac{C_8}{C_9 \cdot [\text{H}^+]_0 + C_{10}}$$

(d) If $[\text{H}_2\text{O}_2]_0$ is varied and the other variables are held constant, a plot of v_0 vs. $[\text{H}_2\text{O}_2]_0$ should fit the following equation:

$$v_0 = \frac{(k_5 k_6 K_1 K_2 K_3 K_4 [\mathbf{A}_{\text{ox}}]_0 [\mathbf{Ru1}]_0) \cdot [\text{H}_2\text{O}_2]_0}{(k_6 K_1 K_2 K_3 [\text{H}^+]_0 [\mathbf{A}_{\text{ox}}]_0 + k_6 K_1 K_2 K_3 K_4 [\mathbf{A}_{\text{ox}}]_0 + k_5 K_1 K_2 K_3 K_4) \cdot [\text{H}_2\text{O}_2]_0 + (k_6 K_2 [\text{H}^+]_0 [\mathbf{A}_{\text{red}}]_0 [\mathbf{A}_{\text{ox}}]_0 + k_6 [\mathbf{A}_{\text{ox}}]_0^2 + k_6 K_1 K_2 [\text{H}^+]_0 [\mathbf{A}_{\text{ox}}]_0)}$$

$$v_0 = \frac{C_{11} \cdot [\text{H}_2\text{O}_2]_0}{C_{12} \cdot [\text{H}_2\text{O}_2]_0 + C_{13}}$$

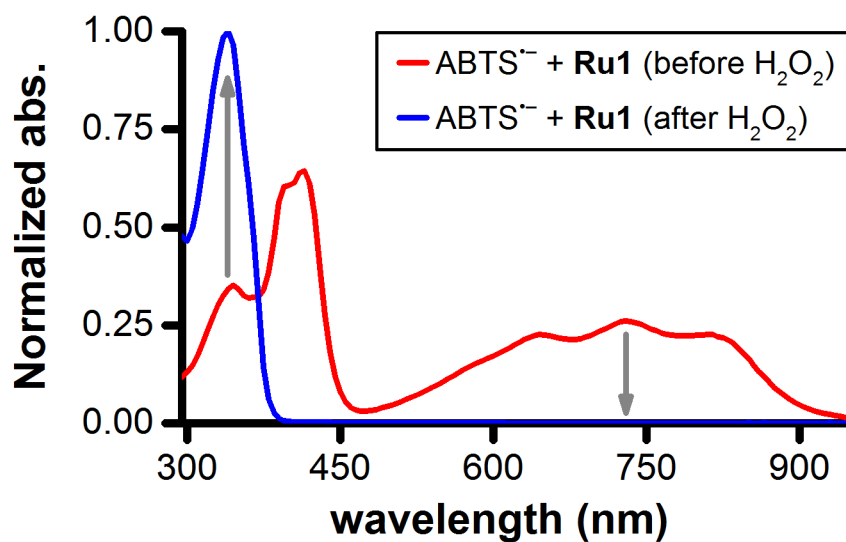
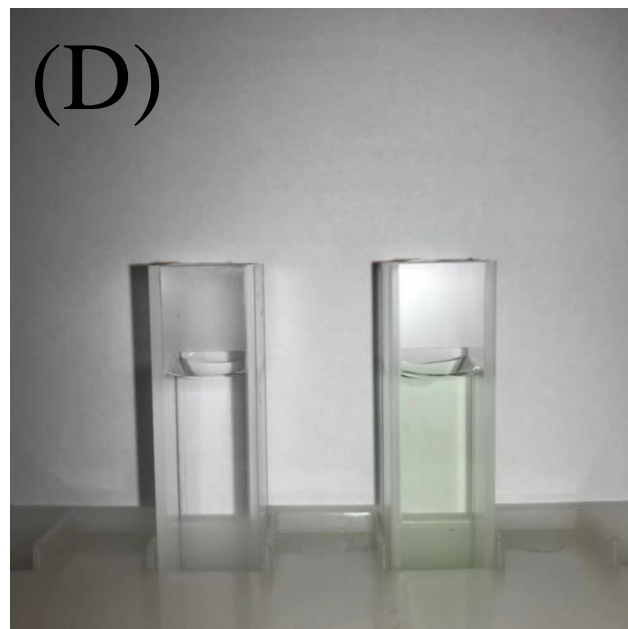
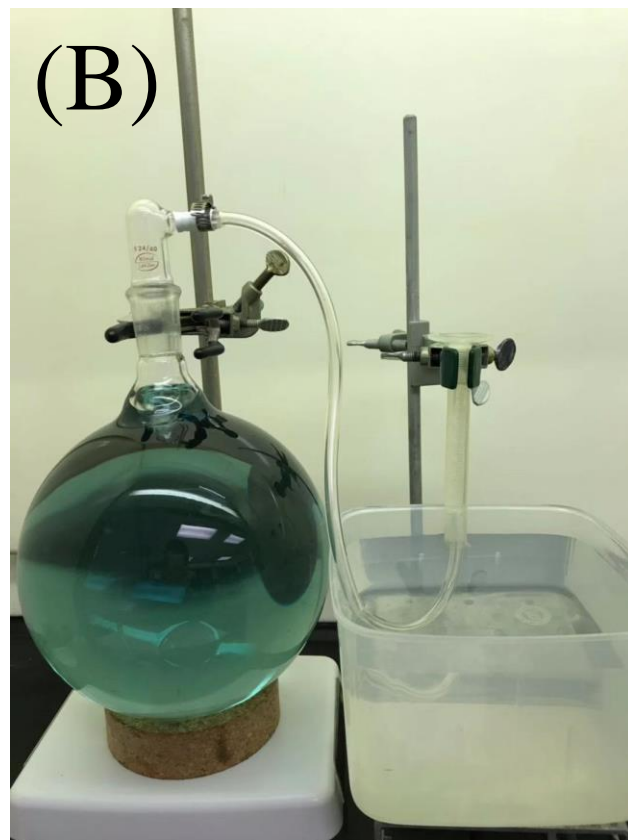
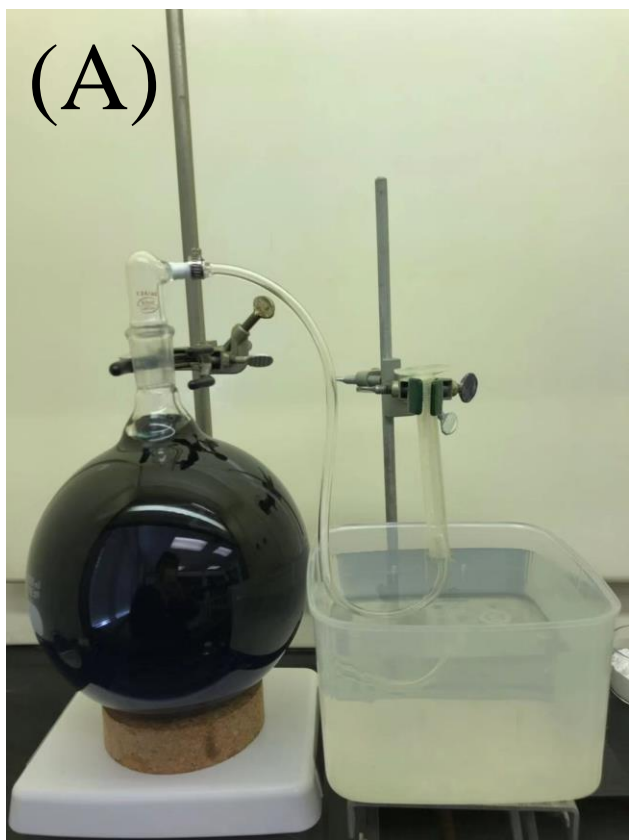


Figure S1. Overlaid UV–visible spectra for ABTS^{•-} + **Ru1** before (red line) and 30 min after the addition of H₂O₂ (blue line). During the course of this reaction, the ABTS^{•-} concentration decreased by 50 μM (downward grey arrow) and the ABTS²⁻ concentration increased by 50 μM (upward grey arrow). Conditions: [**Ru1**]₀ = 5 μM, [ABTS^{•-}]₀ = 50 μM, [H₂O₂]₀ = 100 μM, PBS (pH 7.4), 25 °C; [ABTS^{•-}] determined from absorbance at 734 nm ($\epsilon = 1.5 \times 10^4 \text{ M}^{-1} \text{ cm}^{-1}$) and [ABTS²⁻] determined from absorbance at 340 nm ($\epsilon = 3.7 \times 10^4 \text{ M}^{-1} \text{ cm}^{-1}$).



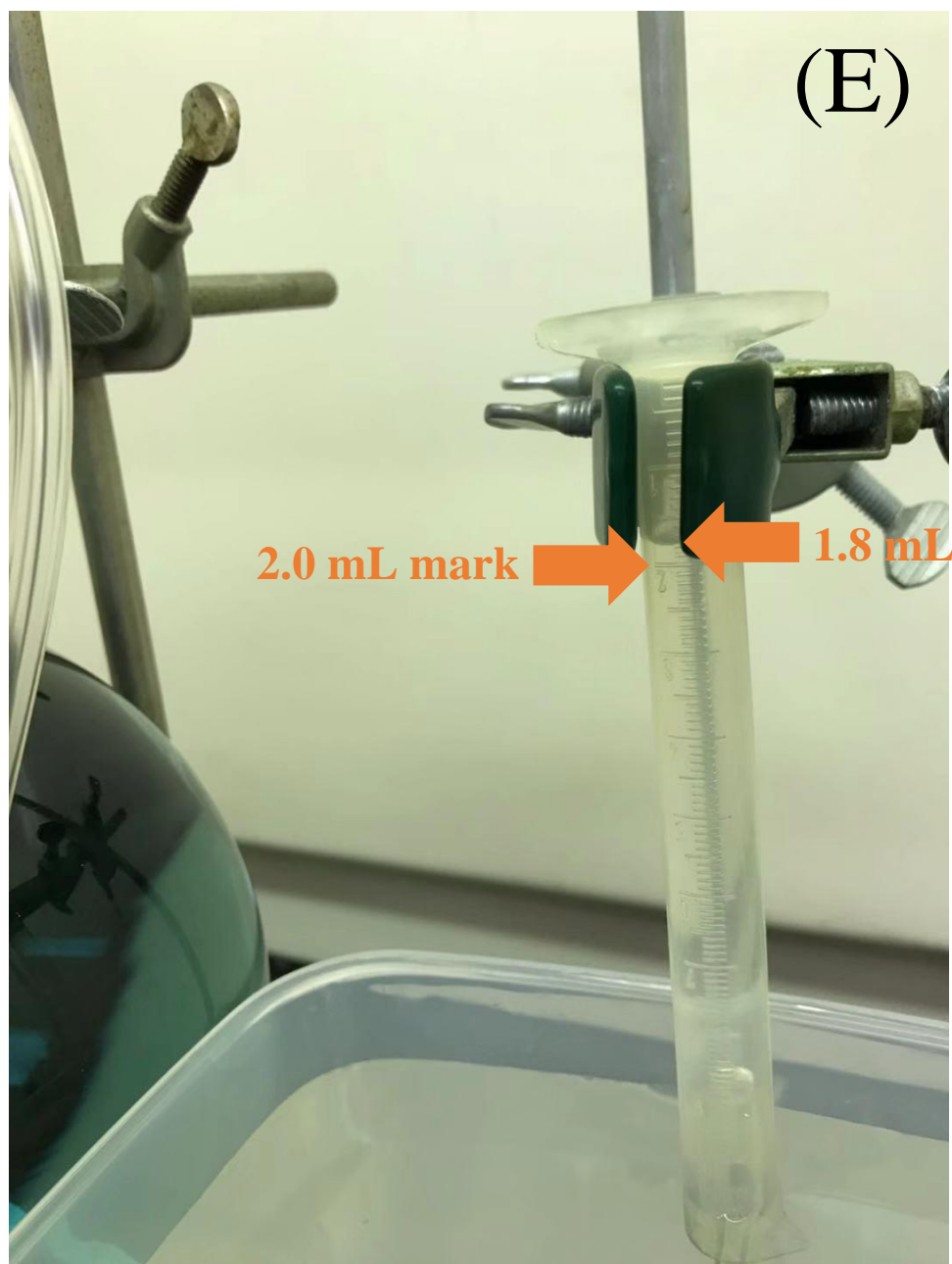


Figure S2. Representative digital images acquired during volumetric measurements of O_2 gas evolution from **Ru1**-catalyzed $\text{ABTS}^{\cdot-}$ reduction with H_2O_2 under standard conditions in 3.00 L reaction volumes. Entire apparatus (**A**) before and (**B**) 30 min after the addition of H_2O_2 . (**C**) Cuvettes containing PBS blank (left) and 3.0 mL aliquot from 3.0 L reaction solution before the addition of H_2O_2 (right). (**D**) Cuvettes containing PBS blank (left) and 3.0 mL aliquot from 3.0 L reaction solution 30 min after the addition of H_2O_2 (right). (**E**) Zoom-in of inverted graduated cylinder 30 min after the addition of H_2O_2 into which $1.8 \text{ mL} \pm 0.1$ of O_2 gas ($72 \pm 2 \mu\text{mol}$) had been collected. Conditions: $[\text{Ru1}]_0 = 5 \mu\text{M}$, $[\text{ABTS}^{\cdot-}]_0 = 50 \mu\text{M}$, $[\text{H}_2\text{O}_2]_0 = 100 \mu\text{M}$, PBS (pH 7.4), $19 \text{ }^\circ\text{C}$, $V_{\text{rxn}} = 3.00 \text{ L}$.

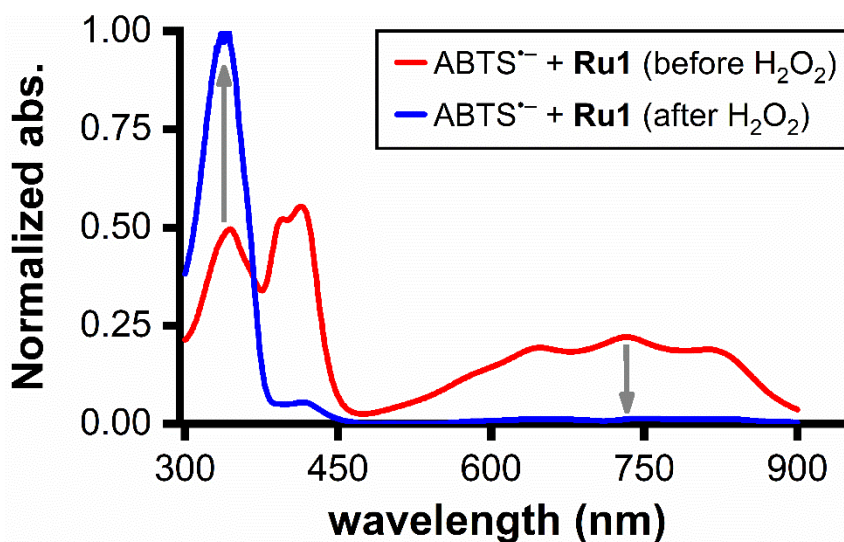


Figure S3. Overlaid UV–visible spectra, of the 3.0 mL aliquots from the volumetric measurements of O₂ gas evolution shown in Figures S2C and S2D, for ABTS^{•-} + **Ru1** before (red line) and 30 min after the addition of H₂O₂ (blue line). During the course of this reaction, [ABTS^{•-}] decreased by $44 \pm 1 \mu\text{M}$ (downward grey arrow) and [ABTS²⁻] increased by $42 \pm 1 \mu\text{M}$ (upward grey arrow). Whereas ABTS^{•-} reduction was quantitative at 25 °C (see Figure S1), at 19 °C it was incomplete (this figure). Accounting for the original volume of 3.00 L shown in Figures S2A and S2B, $132 \pm 3 \mu\text{mol}$ of ABTS^{•-} were reduced to $126 \pm 3 \mu\text{mol}$ of ABTS²⁻, which was accompanied by the evolution of $72 \pm 2 \mu\text{mol}$ of O₂ gas. Thus, for every 1.0 equiv. of ABTS^{•-} reduced, 0.95 ± 0.03 equiv. of ABTS²⁻ were formed and 0.54 ± 0.02 equiv. of O₂ gas were released. Conditions: [Ru1]₀ = 5 μM, [ABTS^{•-}]₀ = 50 μM, [H₂O₂]₀ = 100 μM, PBS (pH 7.4), 19 °C, $V_{\text{cuvette}} = 3.00 \text{ mL}$; [ABTS^{•-}] determined from absorbance at 734 nm ($\epsilon = 1.5 \times 10^4 \text{ M}^{-1} \text{ cm}^{-1}$) and [ABTS²⁻] determined from absorbance at 340 nm ($\epsilon = 3.7 \times 10^4 \text{ M}^{-1} \text{ cm}^{-1}$).

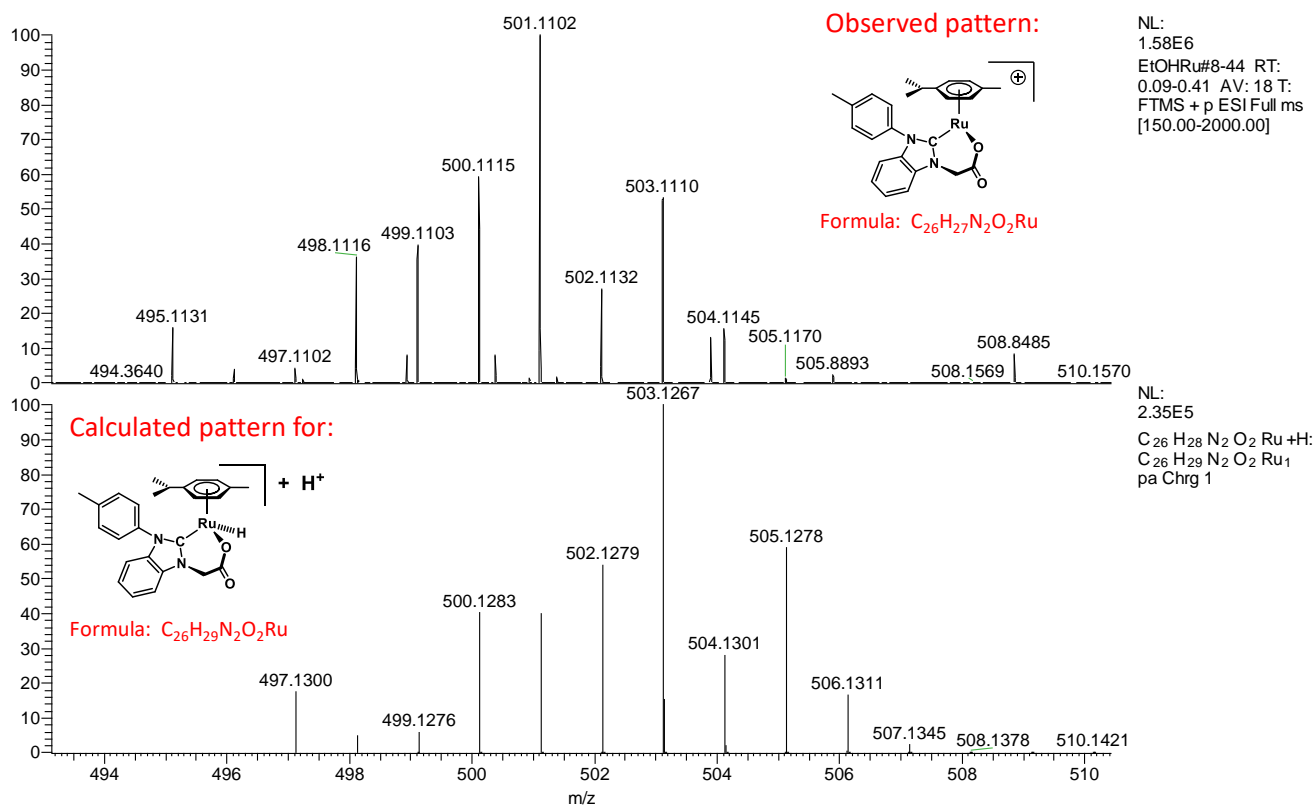


Figure S4. Fourier-transform high-resolution mass spectra with electrospray ionization (ESI-MS) for **Ru1**-catalyzed $ABTS^{\bullet-}$ reduction with H_2O_2 . Samples were administered by direct injection and detected in positive mode. Bottom: calculated pattern for the protonated Ru–H intermediate, which would have the formula $C_{26}H_{29}N_2O_2Ru$. Top: observed pattern in the expected region for the protonated Ru–H intermediate, which does not match calculated pattern, but instead corresponds to a cationic Ru-containing species bearing only the cymene and NHC ligands, which has the formula $C_{26}H_{27}N_2O_2Ru$. Conditions: $[Ru1]_0 = 5 \mu M$, $[ABTS^{\bullet-}]_0 = 50 \mu M$, $[ABTS^{2-}]_0 = 100 \mu M$, $[H_2O_2]_0 = 100 \mu M$, NH_4OAc buffer (10 mM, pH 7.4), 25 °C.

References

1. Y. Htet and A. G. Tennyson, *Chem. Sci.*, 2016, **7**, 4052–4058.
2. Y. Htet and A. G. Tennyson, *Angew. Chem. Int. Ed.*, 2016, **55**, 8556–8560.
3. R. Re, N. Pellegrini, A. Proteggente, A. Pannala, M. Yang and C. Rice-Evans, *Free Radic. Biol. Med.*, 1999, **26**, 1231–1237.